Air oxidation behavior of nitrogen ion implanted zircaloy-4 at 500 °C

QIAN WAN*
Department of Engineering Physics, Tsinghua University, Beijing, 100084, People's Republic of China
E-mail: wanqian99@tsinghua.org.cn

XINDE BAI
Department of Materials Science and Engineering, Tsinghua University,Beijing,100084, People's Republic of China

XIAOYANG LIU
Department of Engineering Physics, Tsinghua University, Beijing, 100084, People's Republic of China

Published online: 16 September 2005

For its low thermal neutron capture cross-section, good corrosion resistance, and adequate mechanical properties, zircaloy-4 is often specified for engineering use in nuclear industry [1]. It is known that certain modification methods can significantly improve corrosion protection. Recent research has shown that ion beam surface processing (IBP) [2, 3] can improve corrosion resistance. Ion implantation, a kind of IBP, offers the possibility to introduce a controlled concentration of an element to a thin surface layer.

Some researches have reported that the corrosion of zirconium alloys in pressurized water reactors (PWR) proceeds mainly through the oxidation process [4, 5], and that the oxidation resistance of metals can be improved by implanting some elements, such as yttrium [6], lanthanum [7], and cerium [8], however, relatively few works have reported on the oxidation behavior of zircaloy-4 implanted with nitrogen. The aim of this work is to investigate the effect of nitrogen ion implantation on the oxidation behavior of zircaloy-4 at 500 °C. The valence of the elements in the surface layer was analyzed by X-ray Photoelectron Spectroscopy (XPS). The phase structures of the nitrogen implanted zircaloy-4 were examined by Transmission Electron Microscopy (TEM).

The specimens were machined to 10 mm × 10 mm × 1.5 mm from a sheet of zircaloy-4, mechanically polished with 200–1000 grade emery paper, then degreased in acetone and ethanol supersonically, chemically polished in the solution of 5 vol.% HF, 45 vol.% HNO_3, and 50 vol.% H_2O, and rinsed in the city water and de-ionized water subsequently.

Electron transparent TEM thin foil specimen were prepared by means of electron beam deposition on NaCl single crystal chips at a rate of 0.1–0.2 nm/s. The vacuum remained at a pressure more than 1×10^{-4} Pa. The thickness of zircaloy-4 film was real-time monitored by a quartz crystal oscillator. The total thickness of the films was about 55 nm. In order to eliminate the stress induced by electron beam deposition, the thin foil was annealed in a vacuum chamber with pressure more than 1×10^{-4} Pa at 850 °C for 1 hr.

As described above, the manufacture of the 10 × 10 mm^2 samples is different from that of the zircaloy-4 thin films, and as a rule, these different ways may lead to some difference in these two types of samples. However, from the composition of zircaloy-4, it can be concluded that the content of zirconium is more than 98%, almost the same as that of pure zirconium. Besides the manufacturing methods, no difference exists in all other experimental conditions. As a result, the difference between the compositions of these two types of zircaloy-4 samples is slight, and the possible influence of the slight difference on the experimental result can be ignored.

Zircaloy-4 specimens were implanted by nitrogen ion using an accelerator with energy of 300 keV at about 40 °C. The implantation dose ranged from 4×10^{14} to 1×10^{16} ions/cm^2. During implantation, the beam current density was 0.55 μA/cm^2 and the vacuum pressure was kept at more than 1.1×10^{-3} Pa. Subsequently, TEM analysis was performed with a HITACHI H-800 transmission electron microscope to examine the surface character of the zircaoly-4 samples.

The valence of the elements on the surface layer was analyzed by XPS, and then compared with the standard spectra, respectively. The oxidation was carried out at 500 °C in an electron furnace in the air environment, and the weight gain curve was measured every 20 min.

The structure of both the unimplanted specimen and implanted specimens were examined by TEM. Figs 1–4 displayed the surface topographic (left) and selected area diffraction pattern (right) obtained from the as-received zircaloy-4 and the N-ion-implanted zircaloy-4 with the dose of 4×10^{14} ions/cm^2, 2×10^{15} ions/cm^2, and 1×10^{16} ions/cm^2, respectively. Fig. 1 shows the typical polycrystalline structure obtained for the as-received zircaloy-4. Similarly no amorphous phase appeared at the lowest dose of 4×10^{14} ions/cm^2. However, with the increase of implantation dose, the grain

* Author to whom all correspondence should be addressed.

0022-2461
DOI: 10.1007/s10853-005-4545-4

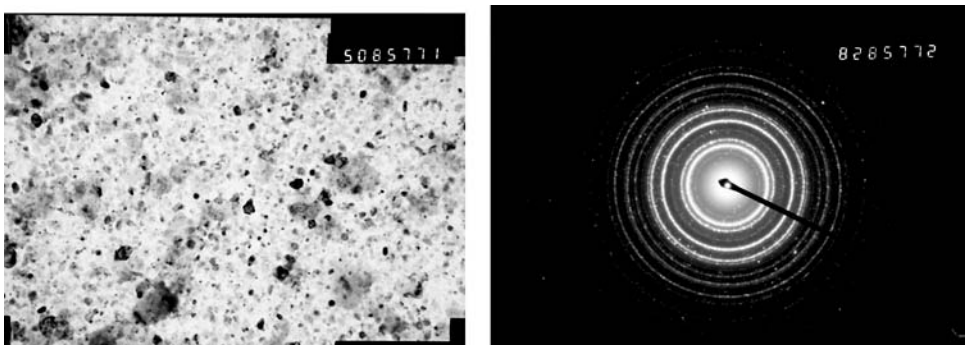

Figure 1 TEM observation of as-received zircaloy4 (left) topographic; (right) the SAD pattern.

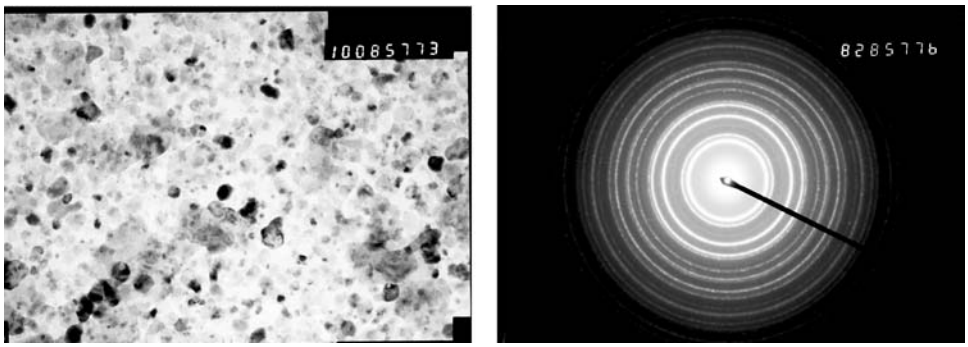

Figure 2 TEM observation of N 4×10^{14} ion/cm^2 irradiated zircaloy4 (left) topographic; (right) the SAD pattern.

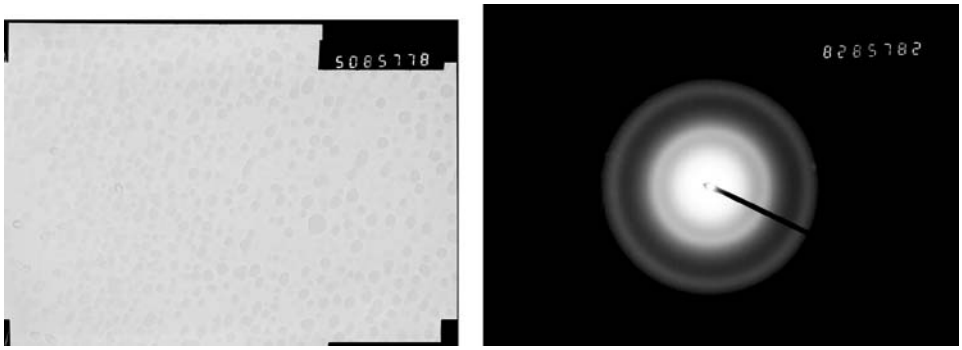

Figure 3 TEM observation of N 2×10^{15} ion/cm^2 irradiated zircaloy4 (left) topographic; (right) the SAD pattern.

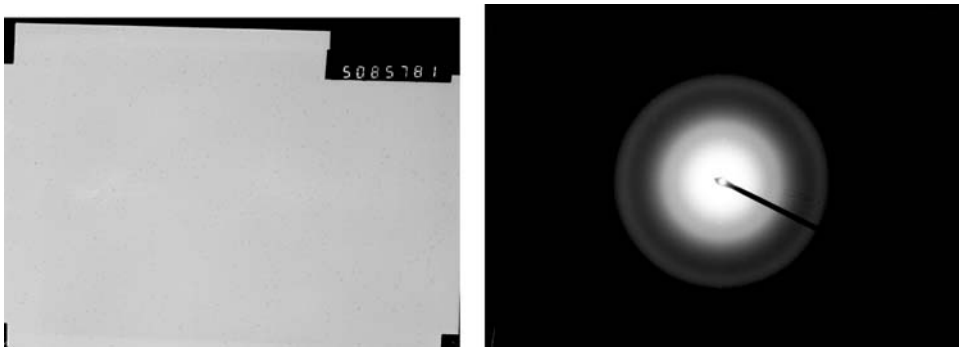

Figure 4 TEM observation of N 1×10^{16} ion/cm^2 irradiated zircaloy4 (left) topographic; (right) the SAD pattern.

size became smaller, the diffraction rings became obscure, and surface structures became amorphous at a dose of 2×10^{15} and 1×10^{16} ions/cm^2.

The composition and the valence of the surface layer before oxidation was analyzed by XPS. Because of the system error in XPS measurement, the energy position should be adjusted by comparing the surface energy of the absorbed C on the surface of the specimen with that of the standard binding energy of 284.8 eV. In Fig. 5, the surface energy of absorbed C on the surface of the specimen is 289.6 eV, which is 4.8 eV higher than the standard binding energy. The adjusted binding energy of the zirconium is 182.2 eV (Fig. 6), which coincides well with the standard value of ZrO_2, so the zircaloy-4 on the surface exists in the form of ZrO_2. Oxygen may come from residual gas in the vacuum chamber, as the

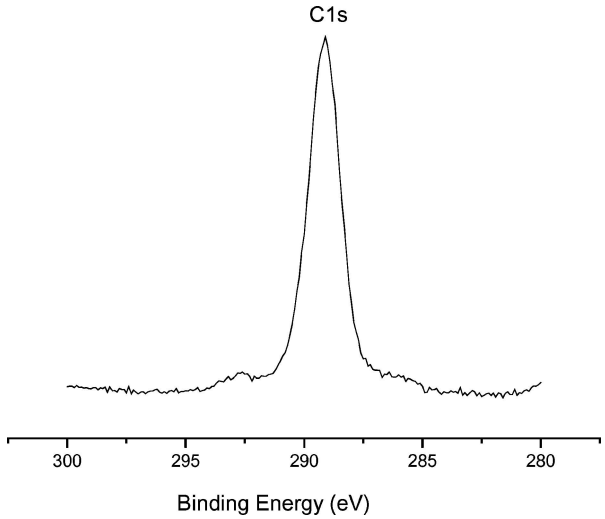

Figure 5 XPS spectra of the C 1s peak in the implanted surface.

vacuum level of the target chamber of the accelerator is not very high.

Weight gain curves of specimens implanted with different doses were shown in Fig. 7. Curve 1# represents the oxidation weight gain of as-received specimen. Curve 2#, 3#, and 4# represent the oxidation weight gain of implanted dose of 4×10^{14}, 2×10^{15}, and 1×10^{16} ions/cm^2, respectively. For each curve, the weight gain increases with the oxidation time. Compared with the oxidation weight gain of as-received specimen (curve 1#), it can be seen that the oxidation weight gain rate of the post-implantation zircaloy-4 specimens increase firstly (curve 2#) and then decrease subsequently (curve 3# and 4#). Such phenomena indicates that when subjected to a low dose (4×10^{14} ions/cm^2), the air oxidation behavior of zircaloy-4 deteriorated, however, with the increase of the implantation dose (2×10^{15} and 1×10^{16} ions/cm^2),

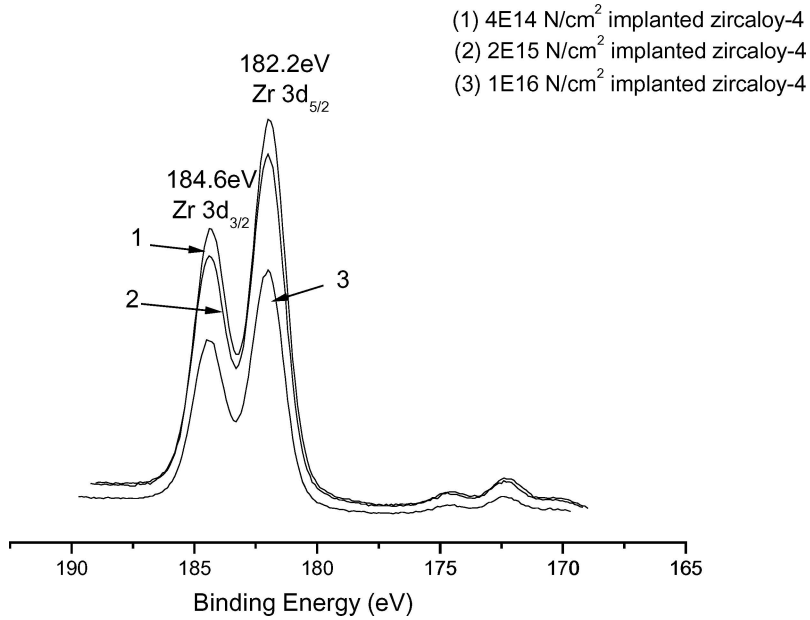

Figure 6 XPS spectra of Zr $3d_{5/2}$ peak in the implanted surface.

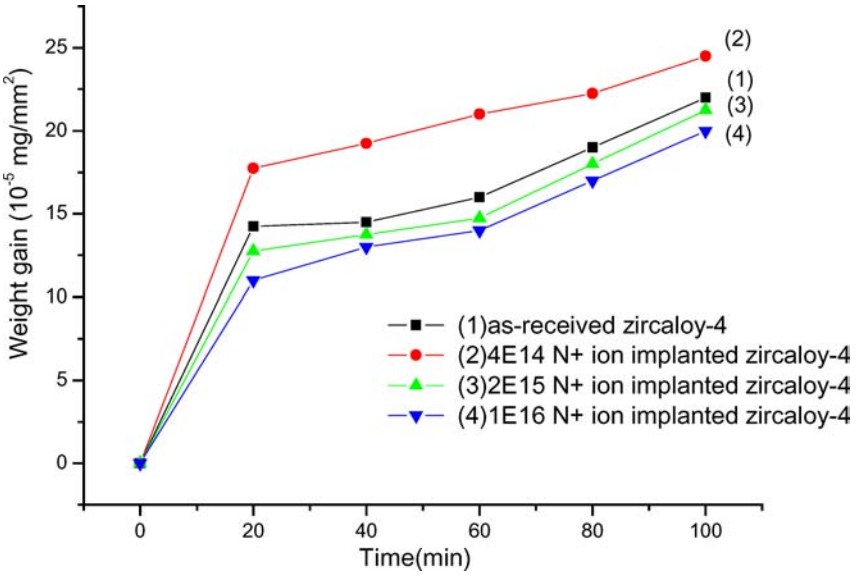

Figure 7 The oxidation weight gain curves for (1) as-received zircaloy-4, and for zircaloy-4 specimens implanted with nitrogen ions at a dose of (2) 4×10^{14} ions/cm^2, (3) 2×10^{15} ions/cm^2, and (4) 1×10^{16} ions/cm^2 at 500 °C in air.

an improvement was been achieved compared with the as-received specimens.

It is well known that, when the target metal was implanted with ions, the surface layer was damaged. Different ion irradiation leads to different damage efficiency. Up to now, many implantation oxidation mechanisms have been proposed such as enhancement of conductivity of an oxide film by a change in energy band under implantation [9], electric conduction of precipitates in the oxide films leading to decomposition [10], and the enhancement of cracks in the oxide film under implantation [11]. The basic effect of implantation is to create a lot of disorder of lattice atoms in the oxide film, which changes the shape of the energy band and add some local conductive states inside the forbidden band along the collision tracks in the oxide films. This is why the oxidation behavior of zircaloy-4 deteriorates when implanted with nitrogen at a dose of 4×10^{14} ions/cm^2. When subjected to a higher dose, an amorphous phase is formed on the surface layer as shown in Figs 3 and 4. It is generally accepted that the oxidation of polycrystalline zircaloy-4 is governed by the diffusion of oxygen along the grain boundaries. Because of the formation of the amorphous phase transformed by nitrogen implantation, grain boundaries which provide preferable oxidation sites were eliminated. As a result, the oxidation behavior of zircaloy-4 was improved compared with as-received zircaloy-4.

In summary, nitrogen ion implantation has significantly changed the oxidation property of zircaloy-4 samples. With an increase of the implantation dose, the weight gain increases first and then deceases quickly. Microstructure analysis of the implanted samples showed that the oxidation behavior at lower dose might be mainly influenced by irradiation damage, while improvement of the oxidation behavior at higher dose could be attributed to the formation of amorphous phase on the sample surface.

Reference

1. P. D. WILSON, "The Nuclear Fuel Cycle From Ore to Waste" (Oxford Science Pbulication, New York, 1996) p. 89.
2. J. JAGIELSKIJ, A. TUROS, G. GAWLIK, *et al*., *Nucl. Instrum. Meth. B*. **127** (1997) 961.
3. M. KLINGENBERG, J. APRS and R. WEI, *Surf. Coat Technol*. **158** (2002) 164.
4. X. BAI, J. XU, F. HE and Y. FAN, *Nucl. Instrum. Meth. B* **160** (2000) 49.
5. F. HE, X. BAI, J. XU, S. WANG, J. AN, Z. SUN and Y. FAN, *J. Mater. Sci. Lett*. **18** (1999) 715.
6. X. W. CHEN, X. D. BAI and J. XU, *et al*., *J. Nucl. Mater.* **305**(1) (2002) 8.
7. D. Q. PENG, X. D. BAI and X. W. CHEN, *et al*., *Surf. Coat. Technol*. **165**(3) (2003) 268.
8. D. Q. PENG, X. D. BAI and X. W. CHEN, *et al*., *Appl. Surf. Sci*. **218**(1–4) (2003) 7.
9. U. STIMMING, *Electrochim. Acta* **31**(4) (1986) 415.
10. P. J. SHIRVINGTON, *J. Nucl. Mater.* **37** (1970) 177.
11. R. A. PLOT, *J. Nucl. Mater.* **91** (1980) 332.

Received 2 February 2004
and accepted 3 February 2005